TNO DIANA
A TNO Company

AUTUMN 2014

DIANA Elements

CONTENT

Colophon

DIANA ELEMENTS *is published by*
TNO DIANA BV
Delftechpark 19a
2628 XJ Delft
The Netherlands

T +31 (0) 88 24262 00
F +31 (0) 88 34262 99

info@tnodiana.com
http://tnodiana.com

DIANA ELEMENTS is distributed to TNO DIANA BV customers and other interested persons.

The editors welcome letters, technical articles, news of forthcoming events, publications of topical interest and project descriptions.

Editorial

Welcome to our Elements magazine which re-emerges at a most exciting time in the history of TNO DIANA. It's been a couple of years since the last Elements Newsletter and with our rapidly growing user base of both academic and commercial customers, a new release seemed appropriate in order to update and inform our loyal customers and Partners alike.

Over the last three years there has been a change of direction and strategy within TNO DIANA following the decision to focus on a fully integrated user interface, controlled by in house developers. Previous years had seen a strong parallel relationship with our good friends at MIDAS and this was a time when DIANA was embedded in their products like GTS while their graphical interface was used for DIANA. While DIANA is still compatible with, and still currently uses FX for DIANA, there has been a significant shift of emphasis internally and the first versions of the new environment came to market in early 2014 in the shape of DIANA 9.5, followed by a further version, 9.6, in November 2014. It is envisaged that by the summer of 2015, DIANA will be fully equipped with its own modelling and meshing capabilities which will allow users to carry out pre and post functions without leaving the same environment.

With the ever increasing need for seismic analysis and fast performance the numerical processing within DIANA has also been upgraded seeing marked improvements in speed and processing ability. A new Paradiso solver, developments on parallel processing and restructuring of the internal processing, in readiness for the new interface, have transformed the analysis available for many of the projects covered by the software. This of course leads to greater efficiency for our customers who can be even more productive with access to the faster results.

DIANA is being utilised more than ever in the domain of Civil and Geotechnical Engineering as well as the Oil and Gas industry and the feedback suggests that we are addressing our target market well with solutions that are both advanced and intuitive. User friendliness is the key to the customers experience we are producing, saving time and allowing modelling to be more efficient. During 2014, another exciting development saw the opening of our own Engineering office in Arnhem, following the appointment of our Director of Engineering ir. Ab van den Bos. Ab has a wealth of experience in both the use of DIANA and practical consultancy work and this knowledge has already seen benefits for our customers who have been helped or guided on various projects by the use of DIANA and the advanced analysis techniques. With expertise in the building and civil domains, and specialised expertise in reinforced concrete, fiber reinforcement and seismic analysis, our customers are finding an additional work force can be beneficial to quickly help them address their Engineering requirements.

In this new edition of Elements, a selection of topical and interesting articles have been compiled for your use which we hope enjoy but also find to be informative.

Steve Owen, Commercial Director

DIANA 9.6 & the Future

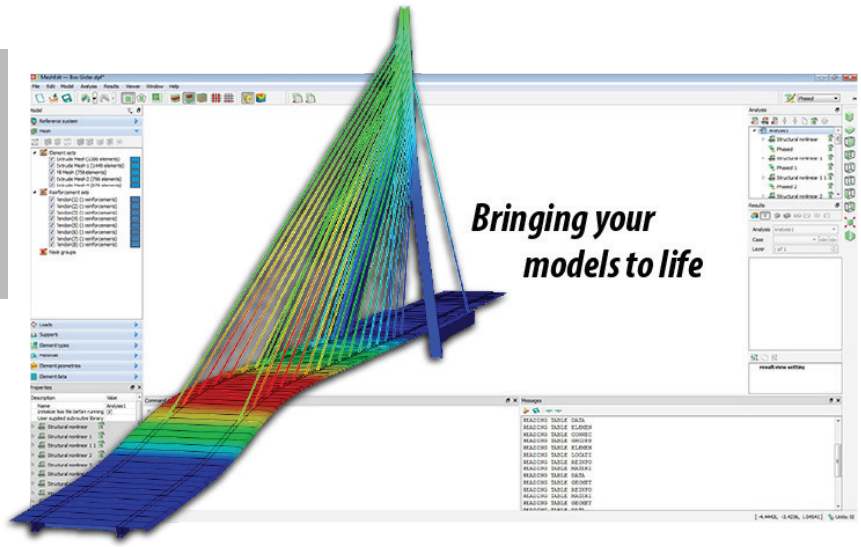

Following the hugely successful release of DIANA 9.5 at the start of 2014 the next stage in the evolution of DIANA, in the form of DIANA 9.6, is ready for release. This release marks a year of development with advances in the graphical environment and further optimisation to the analysis capabilities, providing the user with yet more functionality, modeling and post-processing freedom.

What's New at a Glance...

MeshEditor

- Unlimited undo-redo in graphical environment
- Python scripting console
- Introduction of mesh-sets
- Renewed phased construction analysis
- Renewed spectral response analysis
- Linear constraints
- Extended post-processing options
- Diagram output
- Slice and clipping planes

Element Library

- Element Mesh Topology and Property Assignment
- Reinforcement Mesh Topology and Property Assignment
- Flat Shell Elements
- Analytically Integrated Flat Shell Element
- Structural Interfaces

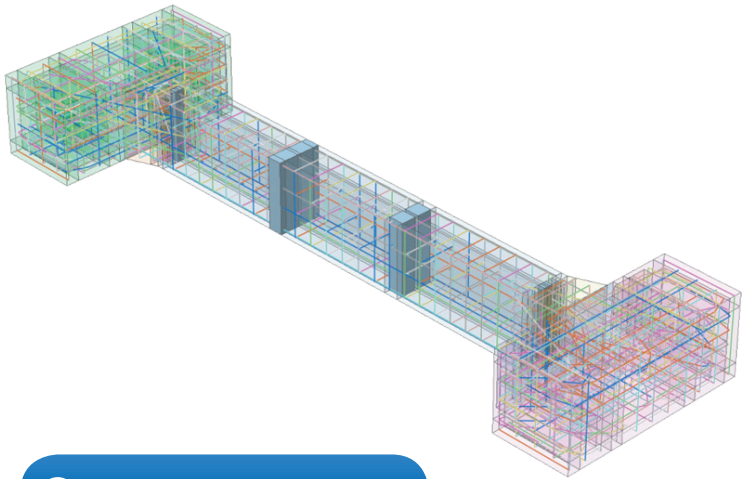

Material Library

- Extension of Total Strain Crack Models based on CEB-FIP model codes 1990 and 2010
- Introducing a new model for tensile failure of fiber reinforced concrete as defined by the CEB-FIB
- Extension in tensile behaviour of Modified Maekawa Concrete Model based on the model code
- Ambient Time Influence on Flat Shell Elements
- Composite Failure Criteria: *Maximum criterion; Tsai-Hill criterion; Tsai-Wu criterion*
- Time and Element Age Dependent Hydraulic Conductivity
- Engineering Liquefaction
- Enhancement in Shima Bond-slip model
- Enhancement in nonlinear behaviour of reinforcement behaviour based on JSCE Concrete Code 2012

Analysis Procedures

- Smart Reinforcement Evaluation
- Smart Composed Element Evaluation
- Initial State Evaluation control option
- Automatic transition of external loads in phased analysis
- Physical Nonlinear Analysis Options
- Eigenvalue Analysis based on FEAST method by using the Intel MKL Extended Eigensolver
- Advancement in Response Spectrum Analysis for large systems
- Superposition of the individual excitation spectra based on Eurocode 8 EN 1998-1
- Maximum Shear Stress output
- Stiffness Adaptation Analysis based on CEB-FIP model codes 1990 and 2010
- Modal Mass output for each eigenfrequency
- Reinforcement Grid Design Checking extension

MORE INFORMATION

What the future looks like...

and Who's Behind It...

The development of the DIANA program was initiated in the mid 70's, which is circa 40 years ago. Since then the program has developed from research software to an analysis tool which is used by engineering consultants, construction companies, research organisations and universities in seventy different countries. The program is used especially for complex analyses such as failure of reinforced concrete, soil-structure interaction with varying and dynamic loadings.

The original strength of TNO DIANA is the Finite Element solver. In 2012 the company decided to invest in the in-house development of a graphical environment for the DIANA solver. Therefore, a new team of developers, with relevant experiences in graphical software, was recruited and as a first step this has resulted in a fully renewed MeshEditor application in DIANA 9.5 launched earlier this year. This graphical environment is specifically designed for the DIANA analysis functionality and combines strengths from other pre-post processors such as iDIANA/FEMGV and FX+ for DIANA. The program will work with both 64-bit Windows and Linux, in both batch and graphical mode. In DIANA 9.6 the post-processing functions have been extended and in 2015 functions for CAD-import, geometrical modelling and meshing will be added. The full work-flow from modelling, analysis and result-checking will be done in the same easy to use graphical environment. When this version is released in 2015, there will also be a version made available for new users.

In recent years the DIANA design functionality has been extended such that material models can be defined with reference to international codes. In addition, the required amounts of reinforcement can also be checked according to these codes. Within the same program a starting user can execute a simple analysis quickly and efficiently and check the design of a structure according to international codes. In the same environment a nonlinear analysis can also be performed (on the same model) where the ultimate limit state is calculated, based on the nonlinear material models and stress re-distribution as a result of material failure.

Because the graphical environment is an in-house development for TNO DIANA, integrated FE-analysis techniques and pre-post-processing operations can easily be modified or added, making it easier for users to execute advanced analyses, or even configure the program for specific applications.

The Development Team at TNO DIANA's Head Office in Delft

Pile Foundation & Tunnel Interaction in Mechanized Shield Tunneling

Mahmoud Seperhamesh
AECOM, New York
Veyra Nasri
AECOM, New York
Navid Allahverdi
AECOM, New York
Maziar Partovi
TNO DIANA BV, Delft

ABSTRACT: This paper presents the methodology and results of comprehensive three-dimensional finite element analyses which were performed to assess the potential impacts of tunneling under an existing subway tunnels as well as potential impact of tunneling under an existing bridge. The finite element models took into account all relevant components of the construction process including the soil behavior, shield tunneling, pre-cast concrete segmental lining and the tail void grouting. The models also accounted for stage construction and detailed shield-driven tunnel boring machine (TBM) processes including applying balancing face pressure as well as injecting bentonite slurry through the TBM shield. This study has demonstrated that the predicted tunneling-induced impacts on the existing structures can be effectively mitigated by using controlled shield-driven TBM tunneling.

1 INTRODUCTION

The main goal of this paper is to present the geotechnical challenges posed in designing an underground light rail transit project in downtown Los Angeles and explain methodology and geotechnical solutions proposed to economically meet these challenges. The project known as Regional Connector Transit Corridor (RCTC) is one of the capital projects envisioned to expand the public transportation in the city of Los Angeles. The preliminary design phase included approximately one mile long 22-ft diameter twin TBM tunnels in soft ground supported by precast concrete segmental lining, three cut-and-cover stations and one mined crossover cavern.

Designing a transit facility in currently congested downtown area brought a collection of design challenges into the picture. The geometrical constraints of connecting two existing stations and cost reduction considerations demanded setting up the alignment in close proximity to existing buildings, structures, and utilities. For example: 1) the proposed alignment passed under an existing operational underground subway line (Red Line) within few feet of vertical separation between tunnels. Raising the proposed alignment so close to the existing tunnels allowed reducing the depth of the adjacent cut and cover stations and hence reducing construction costs. 2) the proposed alignment passed under a bridge (4th Street Bridge) in proximity of piles which are supporting the piers of the bridge structure. The tunnels located within few feet from the piles.

Three dimensional finite element models developed to ensure the minimal impact of tunneling on the adjacent structures. For tunnels crossing under the existing Red Line, it is shown that developed forces and deformation in the lining of the existing tunnels did not exceed the allowable limits. For the case of piles supporting the bridge, the adequacy of load carrying capacity and structural integrity of piles during and after construction of tunnels are ensured. Three dimensional models accounted for stage construction and detailed shield-driven TBM processes including applying the earth balancing face pressure as well as injecting bentonite slurry through the TBM shield.

The original profile was raised such that the vertical separation between the invert of Red Line tunnels and crown of the RCTC tunnels reduced to only about a quarter of the diameter of tunnels. It is evident that reducing the vertical separation between the proposed RCTC tunnels and the existing Red Line tunnels would allow raising the proposed tunnel vertical profile and thereby, result in a reduction in the volume of adjacent station cut-and-cover excava tion. As a result, it was decided to investigate the feasibility of reducing the minimum separation to approximately a quarter of tunnel diameter at the expense of adopting controlled shield driven tunneling to maintain the uninterrupted serviceability of Red Line subway. Earth pressure balance (EPB) shield tunneling was proposed for mining of the RCTC tunnels.

Red line tunnels were built during late 1980's and early 1990's. They consist of twin single-track tunnels with excavated diameter of about 22 ft and variable pillar width between the openings from 13 to 24 ft. The tunnels were excavated using open-face circular shield equipped with a mechanical digger on a rotating arm. The shield was intended to support the ground and allow installation of supports. Tunnel support comprised a two-pass lining; steel rings spaced at 4 ft on center along with wood lagging were used as initial support and a steel reinforced 12 inch thick cast-in-place concrete adopted as final lining. Final lining was cast after completion of the tunnel excavation.

This paper presents the results of a numerical study which was conducted using advanced three-dimensional numerical analysis approach to assess the impact of tunneling-induced ground movements on the Red Line tunnels resulting from raising the proposed bored tunnel vertical profile. Also, the results of a three-dimensional finite element model to assess the impact of tunneling on the piles of the existing 4th Street

Bridge are presented. The proposed profile of the RCTC TBM-bored tunnels at 4th Street Bridge indicated a minimum of 2.5 feet separation between the future tunnels and the existing piles.

2 GEOLOGY AND SUBSURFACE INVESTIGATION

The proposed Metro RCTC alignment is located in the northern portion of the Los Angeles Basin. This basin is a major elongated northwest-trending structural depression that has been filled with sediments up to 13,000 feet thick since middle Miocene time.

The alignment would encounter several geologic units that range in age from Pliocene to recent. The geologic units that would be encountered within the proposed tunnel alignment and station boxes are the Pliocene-age sedimentary strata of the Fernando Formation, Holocene to probable Late Pleistocene Alluvium, and historical/recent artificial fill. Holocene to probable late Pleistocene-age alluvial deposits are present along the alignment beneath variably thick artificial fill. Overlying the Fernando Formation are alluvial deposits comprised primarily of interlayered clays, silts, fine sands, and sand layers containing variable gravel and cobbles. Pliocene-age, sedimentary bedrock was mapped along portions of the alignment. The Fernando Formation is comprised predominantly of massive siltstone, with some interbeds of sandstone and conglomerate and well-cemented, fine-grained silty sandstone. Bedding dip inclinations range from approximately 70 to 75 degrees with dip vectors that range from N168 to N191.

The RCTC project alignment is located within the Los Angeles Forebay Area. Groundwater in the Los Angeles Forebay occurs primarily in the Quaternary age sediments. This is due to the relatively low permeability of the underlying bedrock of the Fernando Formation. Because bedrock is relatively shallow and the water-bearing sediments are relatively thin along the majority of the alignment, only the Semi-perched aquifer is present in the project area. A groundwater level contour map of the Los Angeles Quadrangle indicates groundwater depths ranged from historical highs of about 20 to 50 feet below ground surface. It should be noted that shallow groundwater levels are typically influenced by seasonal rainfall and infiltration in addition to potential localized groundwater extraction.

3 FINITE ELEMENT MODELING APPROACH

The complex and dynamic nature of shield-driven tunnel excavation, staged construction, segmental lining installation process, tail void grouting, and hydro-mechanical coupling in the surrounding ground preclude the use of traditional two-dimensional numerical analysis tools for modeling the ground behavior and structural response for this particular project. Therefore, three-dimensional, non-linear modeling approach, using state-of-the-art analysis program DIANA was adopted to evaluate the ground response and impact of tunneling on existing adjacent structures.

During the past three decades, a vast amount of effort has been expended to numerically simulate the shield-driven TBM tunneling processes and construction operation to accurately estimate the induced ground settlement. Among the latest attempts, Kasper and Meschke (2004) developed a three-dimensional finite element model to study the influence of the soil and grout material properties and the cover depth on the surface settlements, loading and deformation of the tunnel lining and steering of the TBM. They modeled the TBM as a rigid movable body in frictional contact with soil. Their simulations employ a two-field finite element formulation to solve the strain field and pore-water pressure in soil and grout materials. Based on a number of parametric studies, Kasper and Meschke (2006) concluded that: 1) strength characteristics and the over-consolidation ratio are major factors influencing the soil deformation in the vicinity of the shield machine and surface settlements, 2) for soils with a high permeability, larger final settlements observed only after full consolidation was observed, and 3) the cover depth of the tunnel is the most important factor in determining the forces developed in the lining.

The adopted 3D analysis approach allowed modeling the entire geometry of tunnel and excavation staging in order to evaluate the full impact of excavation progression on existing structures.

3.1 Geometry and mesh generation

The perimeter of all excavations was imported from DXF CAD drawings. Once DXF files had been imported, each wireframe was maneuvered into position based on the dimensions provided on the tunnel drawings. The size of the model was determined in such a way to minimize the boundary effects on the analysis results while allowing the analysis to be performed efficiently. In order to model the ground, several points on the estimated top of rock and ground surface were determined based on the available geotechnical information.

The finite element mesh consisting of tetrahedron solid elements was automatically generated. When generating the mesh for RCTC bored tunnels, special attention was paid to the mesh element size in specific areas such as the rock mass region between RCTC and Red Line tunnels. A small element size of 2 ft was used in the vicinity of the tunnels. In other areas with less importance in the rock or soil, the maximum element size was increased to 10 ft.

Careful consideration was also given to the naming of the mesh sets. By assigning a numerical naming system to each mesh set in an excavation sequence, one can use the special stage definition tool provided by the software when generating construction stages, which easily excavates out sets according to numbering. This method is much less labor-intensive for activating and deactivating mesh sets in different stages, especially in models where there can be up to 100 construction stages.

3.2 Procedure for modeling EPB TBM

Applying excavation face pressure and shield bentonite slurry pressure, installing segmental rings, and tail void grouting are among features that were considered in the analysis in order to allow an accurate simulation of the EPB tunneling operations. The TBM excavation advances were modeled in 5 ft intervals which is the length of a segmental ring. The most recent face of excavation was immediately pressurized after excavating each drift in order to reduce the settlement in front of the face. The face pressure was assumed to be constant for ease of application. The applied balancing face pressure was

set equal to the horizontal insitu stress at the center-line of the RCTC tunnels.

In order to model the conical shield support, compression-only gap elements were used to model the conical shield and the variable gap between the ground and the shield. The maximum gap was considered to be 3 inches at the tail of the shield. The length of the shield was assumed to be 15 ft which is equal to three drifts with 5 ft in length. Bentonite slurry pressure was applied through length of the shield, i.e. 15 ft behind the face. This slurry pressure prevents the soil from moving in and reduces the volume of shield ground loss and consequently reduces the ground deformation and settlement. For sensitivity analysis, a range of bentonite slurry pressure values were applied in this study. The slurry pressure values considered include a percentage of the mean insitu vertical and lateral stresses at the center of tunnel. By increasing bentonite slurry pressures, the crown deflection of RCTC tunnels as well as ground convergence would decrease. Theoretically, there is a pressure at which the settlement would completely diminish. Pressures in excess of this value would result in heaving of the surrounding ground.

Precast concrete segmental rings were installed behind the shield. The first 5 ft behind the shield representing the ring under installation was assumed without any support; however, prior rings installed provide full support to the excavation. In addition, the thickness of the segments was assumed to be 10 inches along with 2 inches of hardened backfill grout was considered in the model. A reduction factor of 0.80 was applied to the flexural stiffness of the rings to account for the effects of segment joints as suggested in Lee et al. (2001).

The in-situ stresses were initialized through prescribing at-rest lateral pressure coefficient. Surcharges due to existing buildings were applied as distributed loads on the soil during the initialization stage. All displacements were reset to zero in the initial stage. The three-dimensional analysis was performed by implementing the Construction Stage Stress-Strain Analysis. Mohr-Coulomb failure criterion was adopted for rock behavior. The displacement degrees of freedom at the bottom face of the model were fixed in all directions; however, only out-of-plane displacements were fixed on the four side faces of the model.

4 CROSSING UNDER AN EXISTING TUNNELS

The proposed alignment passed under an existing operational underground subway line within few feet of vertical separation between tunnels. Three dimensional finite element modeling employed to evaluate the settlement under the existing tunnels. The geometry of the tunnel crossing is shown in Fig. 1. The vertical separation between the RCTC and Red Line tunnels was set at five feet after raising the proposed RCTC tunnel vertical alignment to reduce excavation volume of neighboring stations.

The additional stresses and strains induced in the Red Line tunnel lining as a result of RCTC tunnels excavation, were calculated as the difference between the lining stresses/strains determined after the completion of Red Line tunnels and those obtained after completion of the RCTC tunnels construction. The construction sequences of Red Line tunnels were modeled in order to obtain a realistic evaluation of existing stress in tunnel linings before commencing RCTC tunnels construction. As such, the Red Line tunnels were excavated one at a time in 16 ft drifts. CIP concrete linings were installed after finishing the excavations. After installing liners of Red Line tunnels, displacements were reset to zero.

In total, 98 construction stages were defined in the model to represent the construction processes of Red Line and RCTC tunnels. Construction stages from 1 to 22 designated stages for constructing Red Line tunnels, while stages 23 to 98 represented RCTC tunnels construction. The construction operations for the existing Red Line tunnels are simulated by end of stage 22. In this stage the Red Line tunnels are bored and the cast in place concrete lining is installed. The displacements after implementing stage 22 are reset to zero and the principal tensile and compressive stresses are recorded in order to compare with the results obtained from the final stage of RCTC tunnels construction.

The induced principal tensile and compressive stresses are respectively presented in Table 1 and Table 2 for different bentonite slurry pressures. The induced stresses in the Red Line tunnel lining are a function of slurry pressure since all other parameters in the model remain unchanged. Different slurry pressure values correspond to 0, 80, 90, 100, and 110 percent of the mean insitu vertical and lateral stresses at the center of tunnel. For example, as shown in Table 1 and Table 2, the induced principal tensile stress is 35 psi and the induced principal compressive stress is 20 psi for Case 2 in which slurry pressures reach 52 psi. It is noteworthy to mention that all tensile stress readings correspond to the invert of the Red Line lining located just above the RCTC tunnels; while compressive stresses are measured at the crown of Red Line lining above the RCTC tunnels.

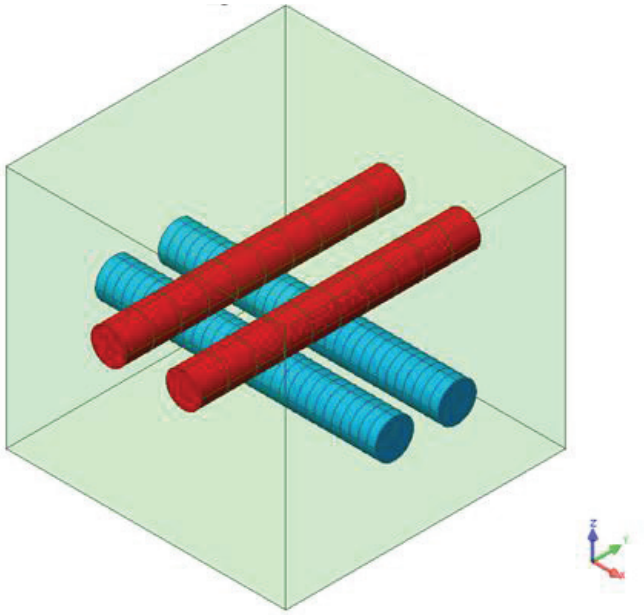

Figure 1. RCTC tunnels (blue) shown beneath the Red Line tunnels (red)

In addition to induced stress/strains developed in the Red Line tunnel lining, the amount of maximum settlement/heave occurred at the invert of Red Line was critical for assessing the potential level of damage to the Red Line tunnels. The deformation readings at the final stage are exclusive to the RCTC tunneling since all displacements prior to RCTC construction were reset to zero. The maximum vertical settlements at the invert of the Red Line tunnels were

compared for all bentonite slurry pressure cases. Table 3 summarizes the maximum deflection at the crown of the RCTC tunnels and the maximum settlement at the invert of Red Line tunnels. A positive value indicates upward movement (heave). Figure 2 shows the profile of settlement along the invert of the existing Red Line tunnels for different values of bentonite pressure. As observed, RCTC excavation can be performed with negligible settlements developed under the Red Line provided proper amount of slurry pressure is applied. Cases 2 and 3 are representing bentonite pressures that resulted in y small settlements in the Red Line invert.

Case No	Slurry pressure	Tensile stress before RCTC	Tensile stress after RCTC	Induced tensile stress
	(psi)	(psi)	(psi)	(psi)
1	0	357	457	100
2	52	357	392	35
3	58	357	388	31
4	65	357	384	27
5	71	357	377	20

Table 1. Tunneling-induced principle tensile stress at the invert of Red Line tunnel lining

Case No	Slurry pressure	Compressive stress before RCTC	Compres-sive stress after RCTC	Induced tensile stress
	(psi)	(psi)	(psi)	(psi)
1	0	330	373	43
2	52	330	350	20
3	58	330	352	22
4	65	330	355	25
5	71	330	356	26

Table 2. Tunneling-induced principle compressive stress at the crown of Red Line tunnel lining

Case No	Slurry pressure	Deflection at crown of RCTC tunnels	Settlement at in-vert of Red Line tunnels
	(psi)	(in)	(in)
1	0	- 0.30	- 0.20
2	52	- 0.07	- 0.02
3	58	0.00	+ 0.02
4	65	+ 0.04	+ 0.06
5	71	+ 0.09	+ 0.11

Table 3. Maximum vertical displacement

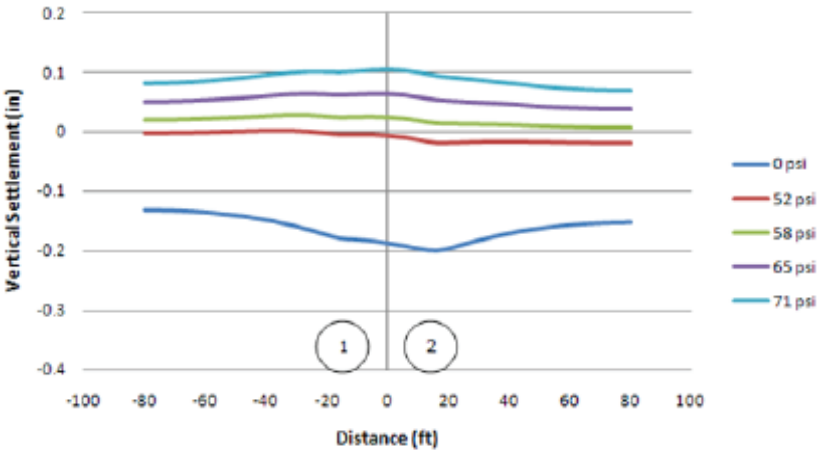

Figure 2. Predicted Settlement/heave along the invert of Red Line tunnels for different slurry pressure

5 CROSSING UNDER AN EXISTING BRIDGE

The proposed RCTC alignment runs between the axes 2, and 3 of 4th Street bridge piers and columns along Flower Street as shown in Fig. 3. The piers and columns of the bridge are resting on deep foundations including piles and caissons. Soil movement as a result of tunnels excavation induces additional forces in the piles. The additional forces may potentially distress the structural integrity of the piles.

The proposed profile of the RCTC TBM-bored tunnels at 4th Street Bridge indicated a minimum of 2.5 feet separation between the future tunnels and the existing piles. It is evident that small separation between the bored tunnels and the existing piles will result in a reduction of skin resistance and tip bearing capacity of the piles depending on the relative location of tunnels with respect to the pile. Any reduction in load carrying capacity of the piles can jeopardize the integrity of the supported structure.

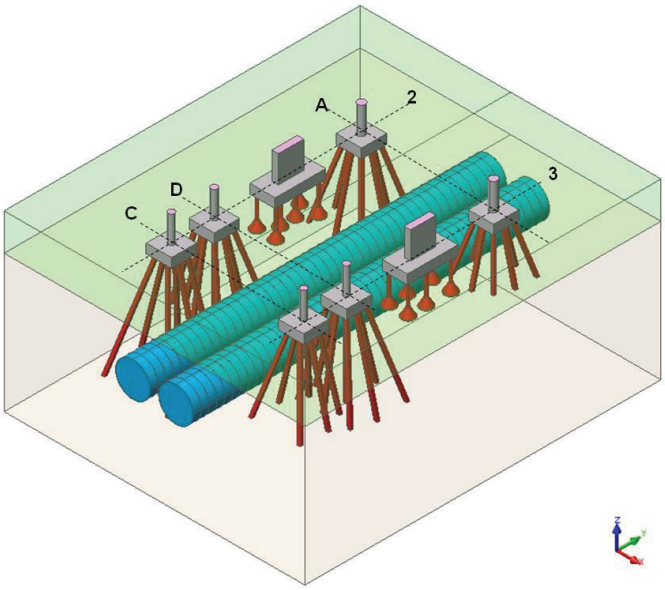

Figure 3. Sketch of RCTC and piles of 4th Street Bridge

This section presents the results of advanced 3D numerical studies which were conducted to assess the impact of tunneling-induced ground movements on 4th Street Bridge piles. The results of a study on the effectiveness of applying bentonite slurry pressures in controlling the ground movement were compared with the case where no bentonite slurry was applied.

The tunneling excavation causes relative axial and lateral deformations in piles located close to the tunnels. The maximum lateral deformation in the pile occurs about the depth of the tunnel's springline as the surrounding soil medium converges toward the center of the tunnel. As detailed in Chen et al. (1999), the vertical soil movement above the tunnel's springline generally is downward and tends to impose negative skin friction on the pile, causing settlement and possible reduction in the pile loadcarrying capacity; however, the vertical soil movement below the tunnel's springline is upward and will cause pile heave. As a result of pile deformation, additional axial force and bending moments will be induced in the piles. The key factor in pile's response and induced forces is the ratio

of pile length to the tunnel cover depth. The pile behavior is rather different for long piles (piles whose tip is below the tunnel's springline) and short piles (piles whose tip is above the tunnel's springline) because maximum soil movements occur about the tunnel springline. In theory, piles in the vicinity of tunneling excavation experience bi-axial moments in both tunneling direction and transverse direction due to deformations resulted from tunneling. These two components of moments can be controlled through pressurizing the face and injecting bentonite slurry through the shield.

The forces induced in piles as a result of RCTC tunnels excavation were calculated from the finite element model and added to the existing service forces in the piles. Service forces are due to the dead load of the superstructure and traffic loads. Additionally, a lateral load equal to 10% of vertical load was considered at the bridge's deck level to account for lateral seismic loads. Analyses were performed for two cases, namely base case and controlled case. In base case no bentonite slurry pressure was considered; while in controlled case bentonite slurry pressure was injected through the TBM shield to limit excavation convergence and consequently mitigate the adjacent piles disturbance. In both cases, TBM face was pressurized.

In following, the results are presented and discussed for settlement of pile-caps as well as forces developed in all pile groups. It is noteworthy to distinguish piles belonging to pile groups of 3A and 2D in interpreting the results. Pile axis designations are shown in Fig 3. Piles in pile group 3A are relatively shorter than piles in the rest of pile groups. They extend only to the tunnel springline elevation; however, piles in other pile groups at least extend about the invert of the tunnels or beyond. Furthermore, piles in pile group 2D have the minimum separation from the tunnels.

5.1 Pilecap settlement and pile forces for base case

The analysis results including settlement experienced under pile-caps, deformation in piles, and forces developed in piles were evaluated in this section for the base case where no bentonite slurry pressure was applied.

Settlements of pile-caps measured less than tenth of an inch at the conclusion of the analysis. The differential settlement of pile-caps was not an issue of concern, since settlement values were quite uniform. Magnitudes of total deformation of piles at the final stage were small and less than tenth of an inch. The largest deformation observed in pile group 3A with shortest piles. Figure 4 shows the magnitude of pile deformations.

The axial force, and bending moment in pile group 2D are shown in Fig. 5, and Fig. 6 respectively. Piles in pile group 2D are rather long piles distinguished with the least separation from the tunnels. The induced axial force and bending moment for base case with no bentonite slurry pressure are presented in Table 4. The final forces induced as a result of tunneling will permanently remain in the piles.

The bending moment reported in Table 4 corresponds to the bending moment associated with pile deformation transverse to the tunneling direction.

Pile group	Axial force under service load	Axial force after RCTC tunneling	Bending moment under service load	Bending moment after RCTC
	(kips)	(kips)	(kips-ft)	(kips-ft)
2A	108.0	287.6	3.40	41.42
3A	115.5	167.3	3.81	48.44
2C	137.6	276.0	6.42	24.41
3C	135.5	290.2	9.03	28.04
2D	107.2	300.2	5.43	32.22
3D	115.1	294.7	6.70	51.21

Table 4. Axial force and bending moment in piles for base case

5.2 Pilecap settlement and pile forces for controlled case

The ground convergence, pile-cap settlements and induced forces in the piles can be controlled via applying pressurized bentonite slurry through the shield. By increasing the bentonite pressure, the tunnel convergence, pile disturbances, and ground settlement will decrease. Theoretically, there is a pressure at which the forces developed in piles as a result of tunneling will be minimal. In this section, the analysis results for controlled case are discussed. In the controlled case, bentonite slurry was injected through the TBM shield. The value of applied pressure was considered as the mean of in-situ vertical and horizontal stresses at the tunnel centerline elevation.

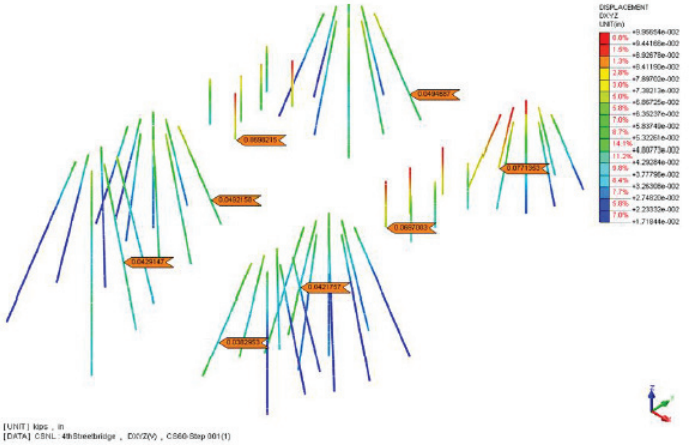

Figure 4. Magnitude of pile deformation after construction of RCTC tunnels (base case)

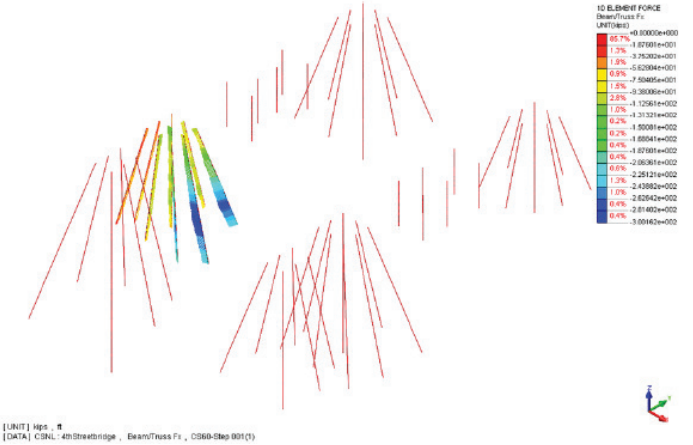

Figure 5. Axial force in pile group 2D after construction of RCTC tunnels (base case)

Figure 6. Bending moment in pile group 2D after construction of RCTC tunnels (base case)

The induced axial force and bending moment for controlled case applying bentonite slurry pressure are presented in Table 5. All induced forces were mitigated as a result of injecting bentonite slurry. Comparing the results of controlled case with those of base case, showed that pile-cap total movements and pile deformations were alleviated by a factor of 2 to 3 as a result of injecting pressurized bentonite slurry. The reduction effects on pile-cap settlements were more pronounced.

Pile group	Axial force under service load	Axial force after RCTC tunneling	Bending moment under service load	Bending moment after RCTC
	(kips)	(kips)	(kips-ft)	(kips-ft)
2A	108.0	205.7	3.40	21.33
3A	115.5	109.8	3.81	25.11
2C	137.6	194.0	6.42	18.24
3C	135.5	199.2	9.03	15.89
2D	107.2	221.7	5.43	17.19
3D	115.1	215.5	6.70	25.21

Table 5. Axial force and bending moment in piles for controlled case

5.3 Pile strength

Structural integrity of piles was investigated for combined effects of axial forces and bending moments. In order to check the combined effects of axial force and bending moments, axial force-bending moment interaction diagram was developed for the pile cross sections. In the as-built record drawings obtained by the project, piles were shown as 26 inch diameter circular section. In design record drawings, it was required for piles to be reinforced at least for the top 20 ft; but no reinforcement was required further below. Maximum axial force and bending moments occurs about the tunnel springline. Tunnel springline is almost 30 ft down the pile height. As such, interaction diagrams were developed for plain concrete section.

Figure 7 shows the ultimate axial and bending moment pairs observed in each pile group for the base case with no bentonite pressure. The ultimate factored forces were obtained by applying a uniform load factor of 1.5 to the results obtained from analysis. As observed, the order of axial force in piles is about the same except for piles in pile group 3A. Based on interaction diagram, the largest demand-to-capacity ratio belongs to pile groups 2D and 3D. The demand-to-capacity ratio is around 0.75. Figure 8 depicts the ultimate axial force and bending moment pairs for the controlled case where bentonite slurry pressure was applied to mitigate the forces. The demand-to-capacity ratio reduced to under 0.60 in the controlled case.

5.4 Pile load carrying capacity

The load carrying capacity of piles was evaluated considering pile tip bearing as well as frictional skin resistance contributions. The forces developed did not exceed the load carrying capacity of piles.

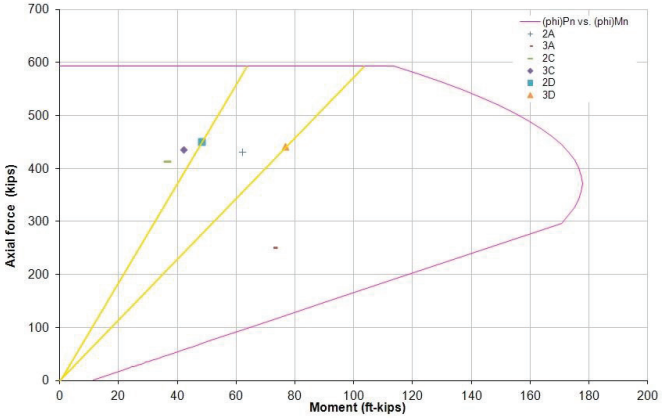

Figure 7. Interaction diagram curve for piles in pile groups (base case)

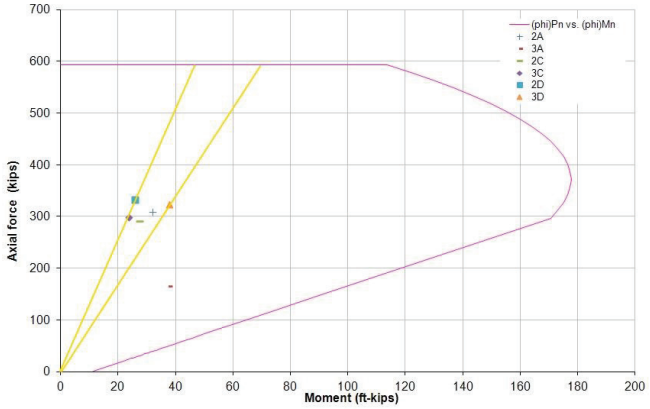

Figure 8. Interaction diagram curve for piles in pile groups (controlled case)

6 CONCLUSION

The objective of this paper is to present the methodology and results of comprehensive three-dimensional finite element analyses which were performed to assess the potential impacts of tunneling under an existing subway tunnels as well as potential impact of tunneling under a bridge.

In order to assess the impact of tunneling-induced ground movements on the existing Red Line tunnels and to investigate the possibility of raising the proposed RCTC tunnel vertical profile, a comprehensive parametric study was conducted which utilized advanced 3D numerical modeling and analysis for Earth Pressure Balance (EPB) TBM driven tunneling. The parametric study of calibrated TBM bentonite pressure was conducted to demonstrate the effectiveness of this measure to mitigate the impacts of tunneling and control ground movements. This study has demonstrated that the predicted tunneling-induced ground settlements under the invert and the stresses/strains in the lining of the existing Red Line tunnels can be effectively controlled by calibrated TBM shield

bentonite pressure. Therefore, it was recommended to raise the proposed tunnel vertical profile to within a quarter of the tunnel diameter (about 5 feet) separation from the existing Red Line tunnels. This recommendation would result in a reduction in the depth of the cut-and-cover excavation for the proposed neighboring stations and consequently, would reduce the cost of construction for these stations.

The results of comprehensive tridimensional finite element models to assess the impacts of boring RCTC tunnels on the foundations of existing 4th street Bridge were discussed and it was shown that the forces developed in the existing piles as results of RCTC tunneling can be safely sustained. It was shown that piles can safely withstand the additional forces due to tunneling via checking the structural integrity of piles as well as the load carrying capacity of piles. The tunneling-induced forces in the piles can be further mitigated via applying bentonite pressure throughout the shield. Also, the deformation of piles and settlements experienced under pile-caps were shown to be negligibly small.

References

Chen, L.T., H. G. Poulos and N. Loganathan [1999]. "Pile Response Caused by Tunneling", J. Geotech. Geoenviron. Eng., No. 125, pp. 207–215.

Kasper, T. and G. Meschke [2004]. "A 3D Finite Element Simulation Model for TBM Tunneling in Soft Ground", Int. J. Numer. Anal. Meth. Geomech., No. 28, pp. 1441-1460.

Kasper, T. and G. Meschke [2006]. "A Numerical Study of the Effect of Soil and Grout Material Properties and Cover Depth in Shield Tunneling", Computers and Geotechnics, No. 33, pp. 234-247.

Lee, K.M. and X.W. Ge [2001]. "The Equivalence of a Jointed Shield-driven Tunnel Lining to a Continuous Ring Structure", Can. Geotech J., No. 38, pp. 461-483.

DIANA [2011]. "DIANA/ User Manual"

Why use DIANA for the Analysis of Tunnels?

DIANA can be utilised in a number of ways in tunnel projects. Analyses normally focus on tunnel induced settlement or lining stress analysis, but DIANA can also be used to research how a tunnel may react in the event of a fire, explosion or even a seismic event.

Now, with increasing congestion in modern cities we are turning even more to underground transportation systems, finding ourselves not only tunnelling under existing structures, but often also under existing tunnels. Ground movement is an inevitable risk to nearby structures which must be carefully assessed, both at the planning stage and as the project unfolds. This, in addition to the potential negative effect on the safety of construction and the project cost, means that the ability to make these predictions accurately is a key. Surface settlement caused by shallow tunnel construction in Greenfield sites can be predicted with some confidence. However, surface settlement in urban areas presents a much more complex interaction between the tunnel and its shafts, the ground and the building.

Using the DIANA software you are able to create detailed 2D and 3D analyses of the interaction between the building, the ground and the tunnel and its shafts. The analysis of existing and new build tunnel linings under the effect of events caused by structural damage, freezing, fire, flood, or earthquake are critical to the safety and longevity of the tunnel. With DIANA, a model of the tunnel segments and joints, along with the soil and grout pressures upon it; and potential factors listed above can be analysed to show intrinsic possible deformations.

Visit our website to find out more about DIANA's capabilities, download our brochure or contact our Sales Team.

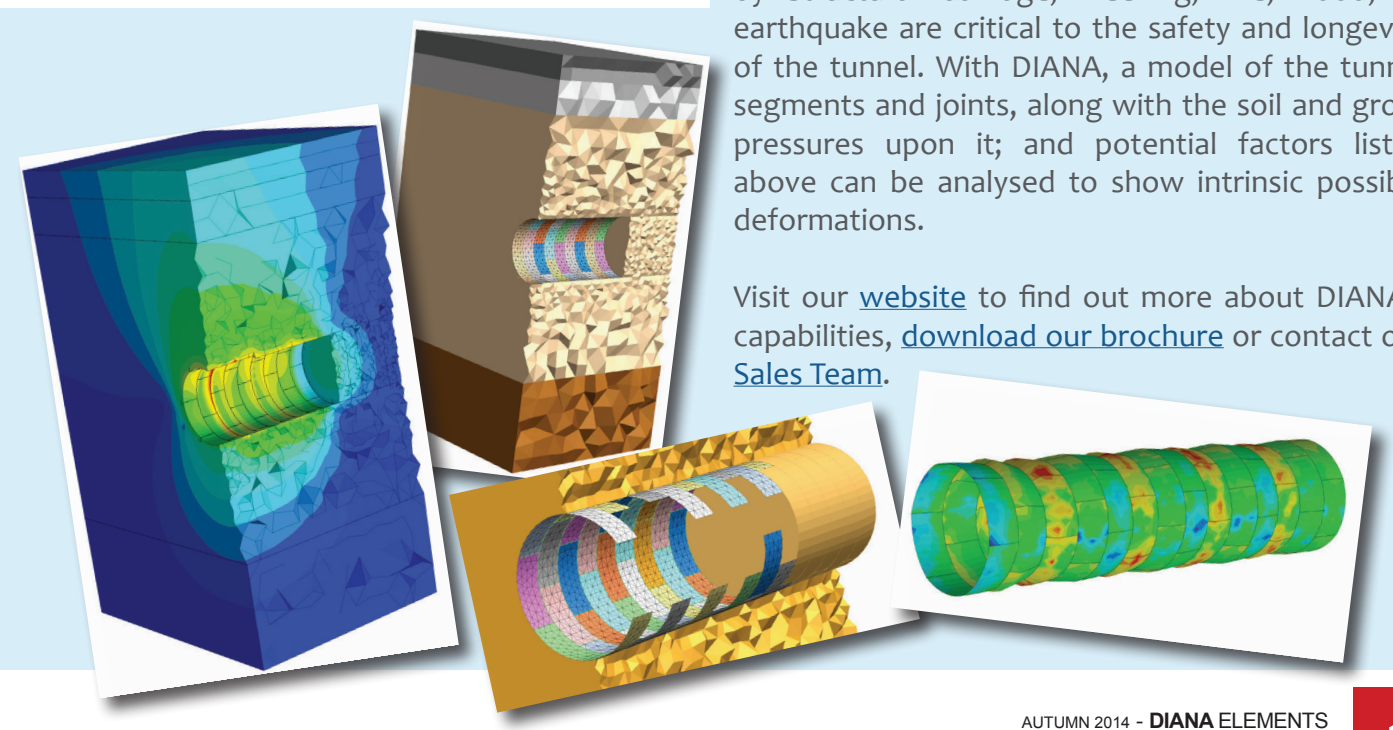

Meet our New Consultancy Team

TNO DIANA BV now offers a new service. The Engineering Consultancy Service gives high value advice for all kinds of engineering analysis.

The main objective is to help engineers who are users, potential users or even non-users, from all over the world with their finite element analyses (FEA). We can demonstrate that the new DIANA environment is still the old powerful open package, but with a totally new user-friendly interface. Modelling is now more straightforward and we can assist engineers at different levels with their projects.

It is possible to model the project from CAD based drawings (BIM) or other input data. Assistance with setting up models is also available.

Sometimes users need guidance on their calculations. In that case, we can make the model and also make the analyses. The user can receive the digital model for learning purposes to reuse in a later phase.

We can also report according to (European) codes. In that way, a report is generated that can be used for the client or as an appendix to a personal report.
Our team is situated in the Netherlands across two offices (Delft and Arnhem), and is extremely well qualified to help you with your projects.

Ab van den Bos is the lead in the consultancy department and has worked for 20 years as a civil engineer. Throughout this period he has been involved in designing projects not only for concrete and geotechnics, but also steel, composites ((G) FRP) as well as other fields. Furthermore, he has been innovating in the joint-less concrete slab market in Europe and also has a lot of experience in forensic engineering. DIANA software is most suitable to assess the remaining strength of a (damaged) structure. Ab is also involved in several (European) technical committees.

Current team members are Chantal Frissen and Pim van der Aa.

Chantal has been working with TNO DIANA since 1996. She is a finite element specialist and knows all about the code of DIANA. She has been working on consultancy projects for many years.
Pim has studied Structural Design at the University of Eindhoven (TU/e) and did his master thesis on modelling SRFC using FEM.

Depending on the project size, it is also possible to pull in extra help from other DIANA specialists within TNO DIANA BV.

If you believe that this is a solution for your future plans then please do not hesitate to contact us (**engineering@tnodiana.com**) with your questions, drawings and background information.

Ab van den Bos
Directeur Engineering

Validation of Seismic Soil-Foundation-Structure Interaction Analysis Procedure for Instrumented Bridges

Anoosh Shamsabadi
California Department of Transport
Maziar Partovi
TNO DIANA BV, Delft

CALIFORNIA DEPARTMENT OF
TRANSPORTATION

ABSTRACT: Instrumented bridges in highly seismic regions are typically supported on complex pile-foundation systems consisting of vertical and battered piles supporting a pile-cap above the mudline. These bridges provide vital transportation links to metropolitan areas, and their closure to traffic in the aftermath of a damaging earthquake can cause debilitating levels of hardship. Recognizing their importance, California Department of Transportation (Caltrans) and California Geological Survey (CGS) have instrumented a number of such bridges, and have been collecting their strong motion response measurements for more than two decades. The deployed instrument sets usually include down-hole sensor arrays, and accelerometers installed on piles, pile-caps, and decks.

Understanding the global Soil-Foundation-Structure Interaction of instrumented bridges is essential to capturing their performance during a major seismic event. In the present study, we model the pile-soil interaction by a series of discrete translational and vertical springs distributed along the pile length and so called "beam-spring" model and to simulate a real nonlinear impact of different soil layers and parameters in conjunction with development of confined stresses on foundation systems and superstructure's behavior in seismic analysis, we need to simulate all these effects in a full scaled model, so called "continuum" model. To this end, we first develop a highly detailed three-dimensional nonlinear finite element model of instrumented bridges in California using both nonlinear beam spring as well as continuum models in DIANA. By applying system identification techniques over recorded motions, as well as recursive and heuristic modeling iterations, we then update theses finite element models, with the specific aim of calibrating the nonlinear continuum model parameters. We finally use the updated model and attempt to quantitatively assess the simplified modeling procedures viz., the beam-spring model and continuum model for seismic design and analysis of bridges.

1 INTRODUCTION

Soil-Foundation Structure Interaction (SFSI) plays a major role in the response of a bridge structure during a seismic event. This paper illustrates the impact of SFSI based on three-dimensional beam-spring and continuum nonlinear dynamic high-fidelity finite-element (FE) modeling analysis for the Samoa Channel Bridge (SCB). SCB is long-span nonstandard bridge located in Humboldt County, California, USA. The particular ground motion for which its model will be calibrated is the January 2010 Ferndale Earthquake. The various components of the nonlinear continuum and beam-spring frame finite element (FE) model are built in the DIANA software platform. We carefully albeit heuristically calibrate the parameters of these models to improve the agreement between the measured and predicted responses.

In the continuum finite element approach, all ingredients of the problem are namely, the structure, foundation, soil, inelastic material responses, radiation damping representing free-field boundary, etc. all explicitly included in a global model as shown in Figure 1and Figure 2. In the, arguably simpler, beam-spring model (Figure 3), the boundary conditions for the foundation system are defined through macroelement models that represent the soil re-sponse. These macroelement models feature back-bone curves (e.g., p-y and t-z curves for lateral and vertical soil reactions), loading-unloading rules to mimic material damping (hysteresis), and gapping capabilities (usually needed for cohesive soils). The beam-spring approach is generally computationally advantageous.

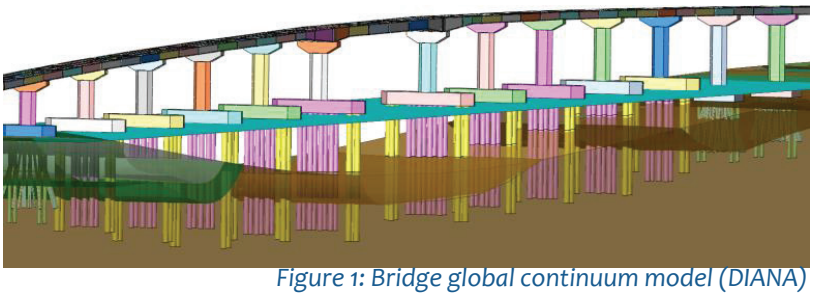

Figure 1: Bridge global continuum model (DIANA)

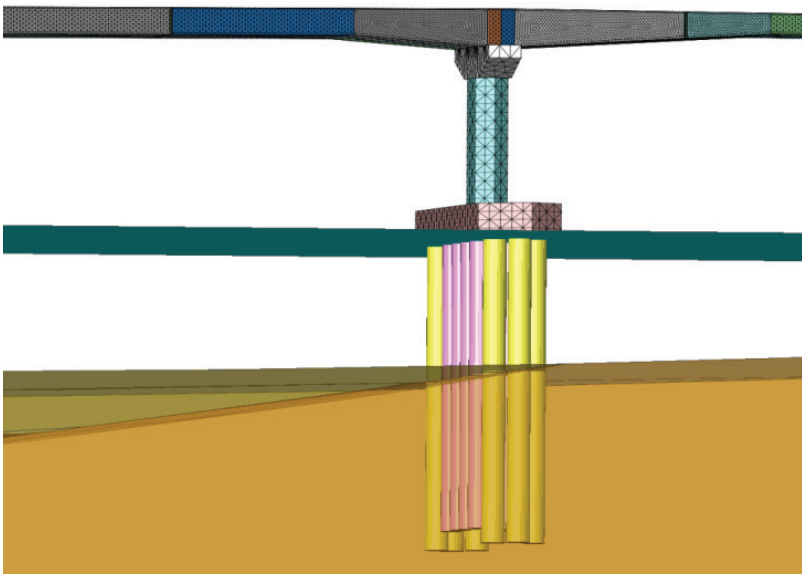

Figure 2: Typical bent with vertical piles continuum model

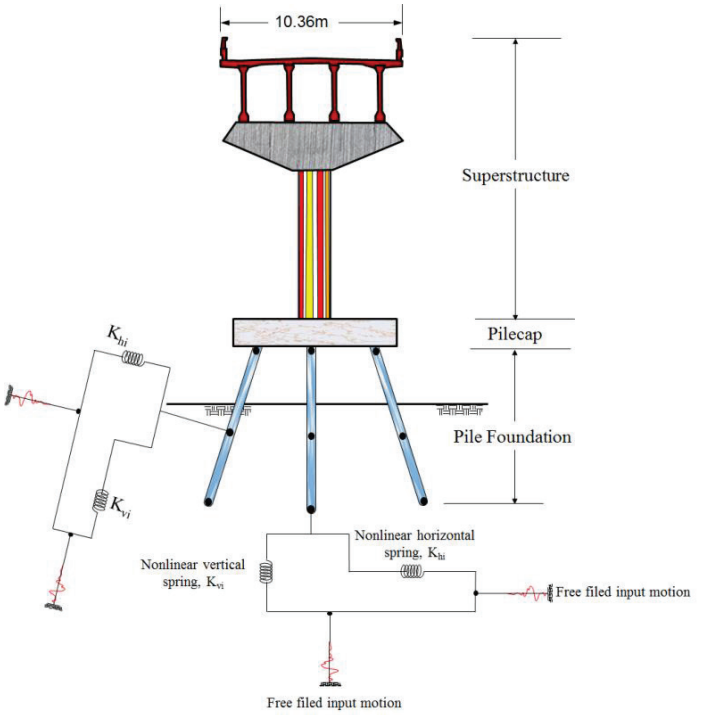

Figure 3: Typical beam-Spring model with battered pile

2 DESCRIPTION OF THE BRIDGE

The Samoa Chanel Bridge (cf. Figure 4) is located in Humboldt County, California (40.822N, 124.169W) and carries Route 225 linking the city of Eureka to Samoa Peninsula. The bridge is approxi-mately 764 m (2506') long and 10.36 m (34') wide (cf. Figure 5). It was constructed in 1971 (construction started in 1968) and underwent a seismic safety retrofit in 2002 (Caltrans, 2002).

The superstructure comprises 6.5" thick (16.5 cm) concrete deck slabs resting on four pre-stressed precast concrete I-girders with intermediate diaphragms (cf. Figure 6). The composite deck is supported on concrete bent-caps and hexagonal single-columns, and seat-type abutments. The bridge consists of a total of 20 spans including the Main Channel crossing.

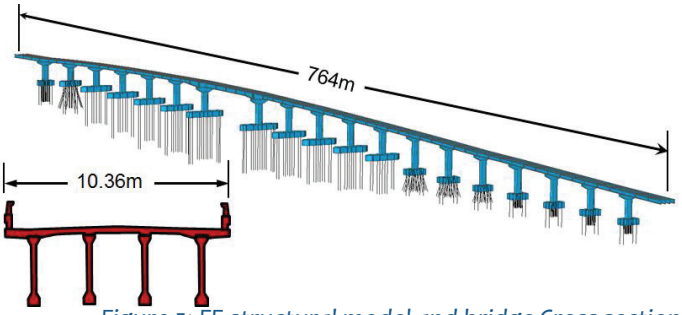

Figure 5: FE structural model and bridge Cross section

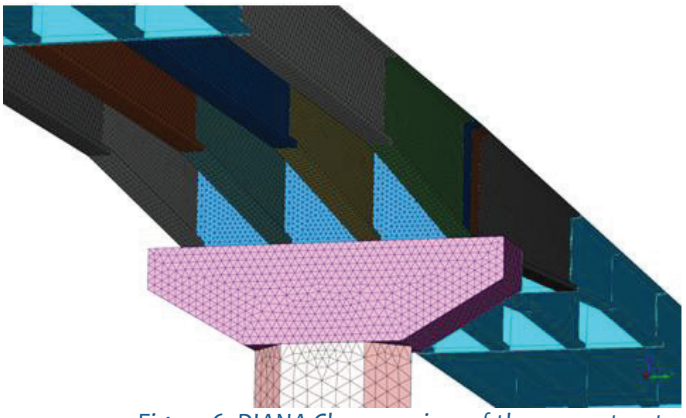

Figure 6: DIANA Close-up view of the superstructure

Figure 4: General view of the Bridge

Typical span length is 120' long (36.6 m) except the main channel, which is 225' long (68.6 m) extending from centerline of pier 8 to the centerline of pier 9. The 150' long (45.7 m) concrete I-girders of the su-perstructure begin at pier 7 and pier 10, and are can-tilevered 30' (9.1 m) past pier 8 and pier 9 into the main-channel crossing span. The 165' long (50.3 m) pre-stressed precast concrete I-girders resting atop the cantilevered portions form the main-channel crossing span (cf. Figure 7 and Figure 8).

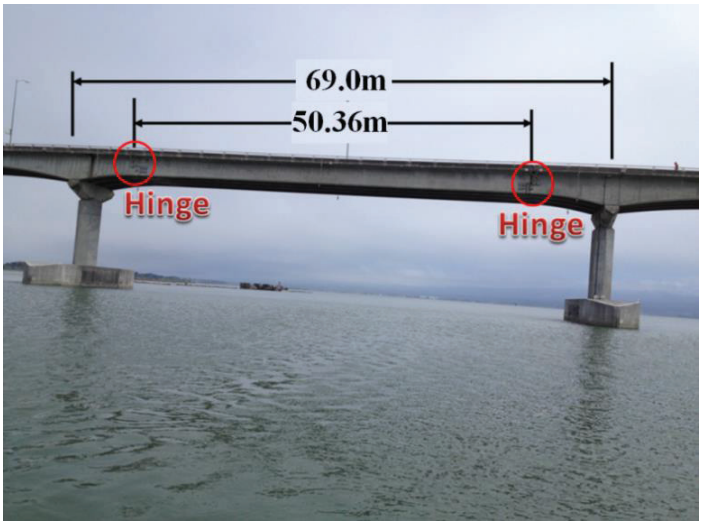

Figure 7: Main shipping channel

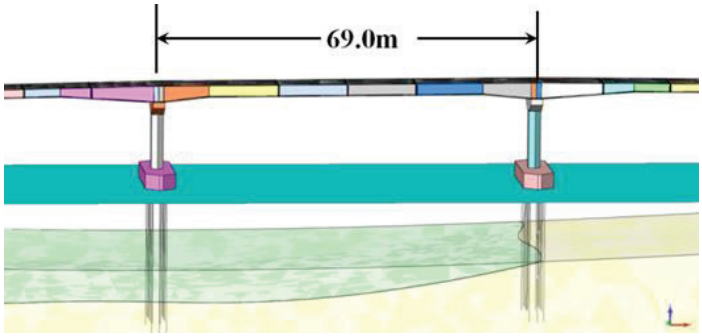

Figure 8: DIANA main channel Continuum model

3 THE FOUNDATION SYSTEM

The bridge is supported on vertical as well as battered pile foundations (cf. Figure 9). The soil underlying the bridge is predominantly a sandy deposit. Depending on the pier location, pile groups consist of 9 to 24 piles. The pile-caps of abutments 1 and 21 (the left and right-ends of the bridge profile shown in Fig. 4) are sitting on original ground. The pile-caps at piers P2 and P14 to P20 are embedded in soil, and the pile-caps from P3 to P13 are above the mudline and at the waterline.

The abutments 1 and 21 are seat-type abutments, and are supported on 12-14" (35.6 cm) square-shaped driven concrete piles. The front row consists of 7 piles battered at a 1:3 ratio and the back row consists of 5 vertical piles. The existing piles at piers P2 and P17 to P20 consist of 16-14" (35.6 cm) square concrete piles driven vertically in a 4×4 square layout. The retrofit piles (cf. Figure 11) con-sist of 4 driven 36" cast-in-steel-shell (CISS) piles with a steel shell thickness of ½" (13 mm) at the four corners of the existing pile layout. There are a total of 20 piles at each one of these piers.

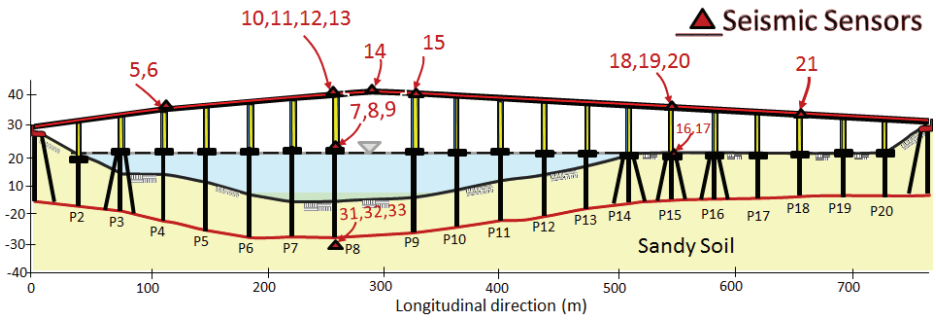

Figure 9: The profile locations of its seismic sensors

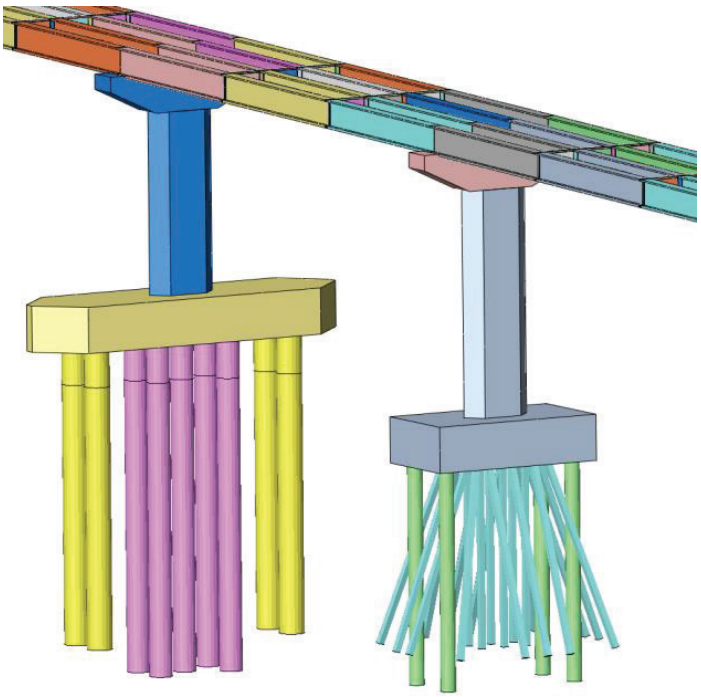

Figure 10: FE model of vertical and battered pile

Piers P3 and P16 originally consisted of 16-14" (35.6 cm) square piles (driven) in a 4×4 layout. The 12 exterior piles were driven at a 1:3 batter, while the 4 interior piles are vertical. The retrofit consisted of driving an additional 4-36" (91.4 cm) CISS piles at the four corners of the existing pile layout. The steel shell is ½" (13 mm) thick.

Piers P4, P5, P6, and P13 each consist of 9 driven vertical piles. The 5 original piles are 54" (1.37 m) hollow concrete piles with a wall thickness of 5" (12.7 cm). The piles were driven in a square formation with 1 pile in the center of the square. For the retrofit, 2 piles on each side of the centerline of column were driven into the soil just outside of the existing pile-cap for a total of 4 retrofit piles. The retrofit piles are 60" (1.52 m) CISS piles with a steel shell thickness of ¾" (19 mm).

The original piles at piers P7 and P10 to P12 consist of 6-54" (1.37 m) hollow concrete piles driven in 2 rows with 3 piles in each row. The 60" (1.52 m) CISS retrofit piles were driven in line with the existing piles creating 2 rows with 5 piles total in each row for a total of 10 piles for these piers. All piles at these piers, existing and retrofit are vertical piles.

Piers P8 and P9, which make up the main channel span, consist of 14 driven piles each. 8-54" (1.37 m) hollow concrete piles are existing piles and 6-60" (1.52 m) CISS piles with a ½ thick shell are retrofit piles. The existing piles were vertically driven in 2 rows with 4 piles in each row. The centerline of each row is 4.5' (1.37 m) away from the center-line of pier. Four (4) of the retrofit piles are driven in line with the existing piles creating a 2×6 layout symmetric about the centerline of pier. The last 2 retrofit piles were driven on the outside of the 2×6 layout in line with the centerline of pier. All retrofit piles are vertical (cf. Figure 11).

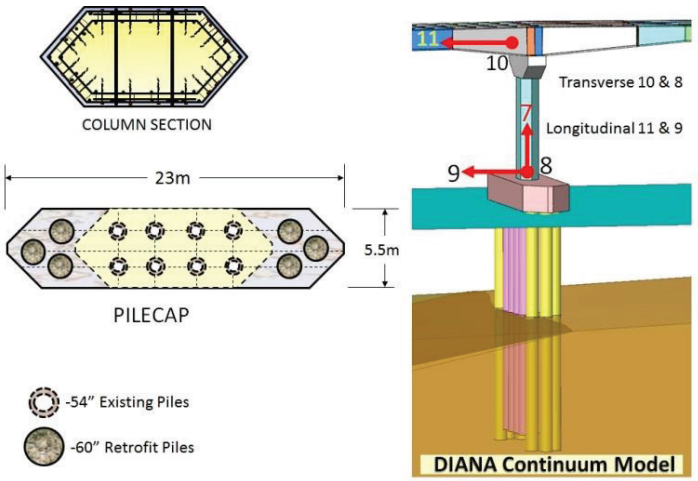

Figure 11: Pier 8 seismic sensors and pile layout

At piers P14 and P15, there are 20 existing 14" (35.6 cm) square-piles driven in 4 rows with 5 piles per row creating a 4×5 layout. The third pile of every row is in line with the centerline of column. The 14 exterior square piles are battered at a 1 to 3 ratio, while the 6 interior piles are vertical. The 4-36" (91.4m) CISS retrofit piles (1/2" i.e., 13 mm thick steel shell) are driven at the corners of the 4×5 layout. The retrofit piles are vertical.

4 INPUT GROUND MOTIONS

The Samoa Channel Bridge was seismically instrumented in 1996, and has suffered several strong earthquakes since. The largest earthquake that shook the structure is the 6.5 Magnitude January 2010 "Ferndale Area" earthquake (source location 40.65N, 124.76W). The location of the instruments that measured free-field motions and the response of the structures at various locations along the bridge are shown in Figure 9. The free-field seismic sensor is located at the bottom of the retrofitted pile. The locations of the seismic sensors at the pile-cap and at the superstructure deck level in both the transverse and longitudinal directions for Pier 8 are shown in Figure 11. The displacement time histories of the input motion and recorded response of the structure in the longitudinal and transverse directions are shown in Figures 12 and 13, respectively. The recorded peak displacement of the free-field motion is about 5 centimeters in the longitudinal direction and peak displacement response of the pile-cap and the deck are about 13 and 15 centimeters, respectively. The recorded peak displacement of the free-field motion is about 3 centimeters in the transverse direction and peak displacement response of the pile cap and the deck are about 8 and 9 centimeters, respectively. The recorded motions in both transverse and longitudinal directions indicate that amplitude of the movement is approximately threefold with respect to the free-field motion.

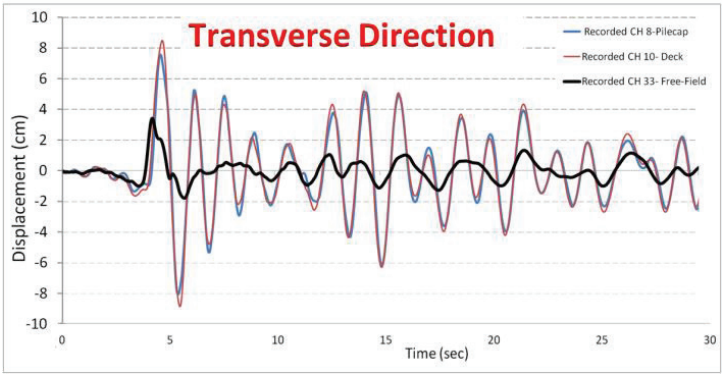

Figure 12: Recorded longitudinal at Pier 8

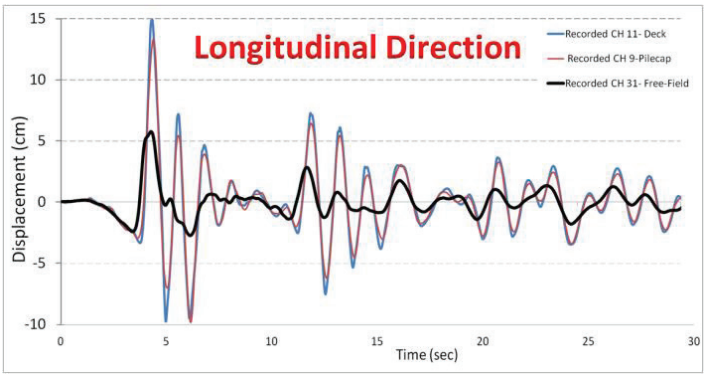

Figure 13: Recorded transverse motions at Pier 8

5 THE BEAM-SPRING MODEL

The configuration of the global beam-spring model of the bridge is shown in Figure 5 and close-up view of a typical bent including superstructure, pile-cap and foundation system is shown Figure 14. The complete beam-spring SFSI model consists of two substructures separated by a foundation interface: (1) superstructure, (2) pile foundation, (3) surrounding soil, and (3) input ground motions. The fully three-dimensional nonlinear model includes all structural components, foundation components, three-component depth-varying nonlinear soil springs and input motions. The nonlinear soil springs (Matlock, 1970; API, 1993) were developed using site-specific geotechnical data (CSMIP, 2012) and bridge plan "Log of Test Borings." The soil springs have nonlinear backbone curves, and display hysteretic response upon unloading.

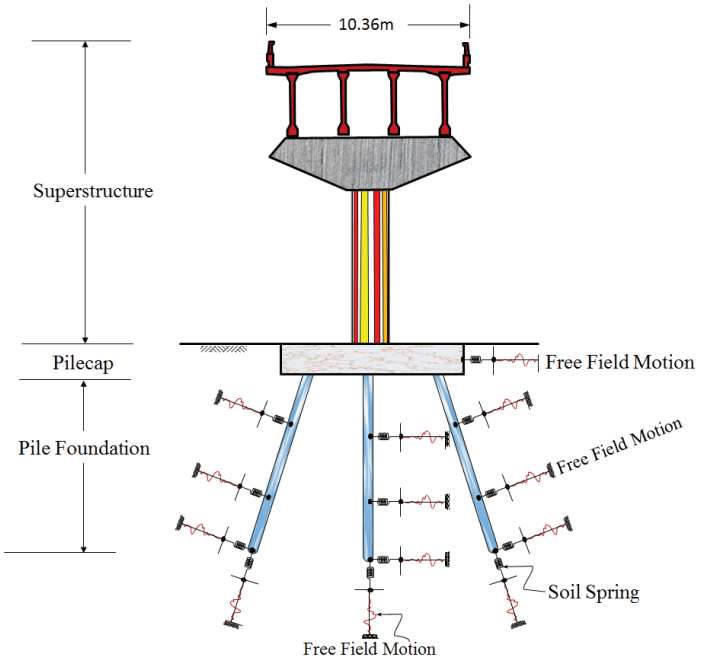

Figure 14: Typical bent nonlinear beam-spring model

Several issues were especially important in matching observed responses of the bridge-foundation system. These were the use of cracked moment of inertia values for the columns and pile elements, and an accurate modeling of the mass of the foundation system. The bridge deck and the pile-caps were modeled with shell elements; the columns were modeled with beam elements. The pile foundations were also modeled with beam elements, but with nonlinear springs attached at discrete locations to represent the lateral and vertical interactions between the piles and their surrounding soil media. The supports provided by the abutments were mod-eled using a "friction isolator" to simulate the elas-tomeric pad, and to decouple the superstructure and abutment backwall from the pile-cap. The

isolator was fixed in the vertical direction only. The longitu-dinal abutment-backfill was modeled by a series of nonlinear link elements distributed along each abut-ment backwall using the experimentally validated formulation provided by Shamsabadi et al. (2010). Those abutment springs were offset by 2.54 cm (1 in.) to take the abutment expansion gap into account.

6 CONTINUUM MODEL

Bridge engineers, by-and-large, used to avoid continuum finite element model analyses carried out with three-dimensional global models because of computational costs. Due to continuous ongoing development in computer technologies (software and hardware) and easy access to high-performance computers, the continuum finite element model method, today, appears to be a feasible approach for investigating and quantifying soil-structure interaction effects in the seismic response of bridges. High-performance computers are now ubiquitous, and modeling a complete continuum-bridge-foundation system and analyzing its (nonlinear) responses in the time-domain using a personal computer are general-ly deemed as feasible tasks. In the continuum FE model, the coupled soil-foundation system columns and the bridge superstructure are developed in a single platform as shown in Figure 11. Advanced non-linear hysteretic models are used for constitutive modeling of the foundation soil, piles and the columns.

In DIANA model solid elements (linear tetrahedron elements) have been used for superstructure, foundation and soil layers. Also beam elements have been used for submerged pile elements as well as embedded pile elements for the parts of the piles, which are embedded into soil layers. Nonlinear plane interface elements have been used to simulate the effect of bearings, shear-keys and connections to abutments (Figure 15). Moreover, embedded line to solid interface elements have been used to depict the nonlinear behavior of pile-soil interactions. In total about 3 million elements have been used (Figure 16).

6.1 Soil Constitutive modeling

Hysteretic behavior of the layers is simulated using Modified Mohr-Coulomb (MMC) soil model. This model include Mohr-Coulomb type yield surface with a non-associative flow rules and a robust hardening rule available in DIANA. For a typical soil layer, the input parameters used for the soil constitutive modeling of the soil are presented in table 1.

Material parameters			
Unit weight γ (kN/m^3)	Initial friction angle φ (deg)	Cohesion c (kPa)	Dilatancy angle ψ (deg)
19	30	0.1	0

Material parameters				
Failure ratio	E_{50} (MPa)	E_{oed} (MPa)	E_{ur} (MPa)	Poisson's ratio ν
0.95	97	116	290	0.3

Table 1. Input parameters for the MMC model used in the finite element simulations.

6.2 Concrete Constitutive modeling

Hysteretic behavior of the reinforced concrete is simulated using the Total Strain Crack model available in DIANA. The input parameters used for the concrete constitutive modeling of the concrete segments are presented in Table 2.

Material parameters				
E (MPa)	ρ (kg/m^3)	f_c (MPa)	f_t (MPa)	G_{fI} (Nm/m^2)
25000	2300	28.5	2.5	0.75

Material parameters			
Crack model	Tensile curve	Compressive curve	Poisson's ratio ν
Rotate	Linear	Thorenfeldt	0.2

Table 2- Input parameters for the Concrete model used in the finite element simulations.

Figure 15: Continuum FE model of bridge structure

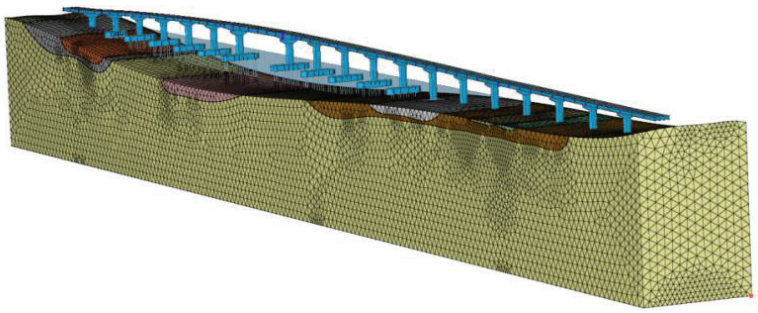

Figure 16: Continuum FE model of soil and structure

7 REPRESENTATIVE RESULTS

Figure 14 displays the primary transverse mode which is dominated by the main channel span computed using the beam-spring and continuum models. This mode has a period of 1.45 seconds for the beam-spring model and 1.38 seconds for the continuum model.

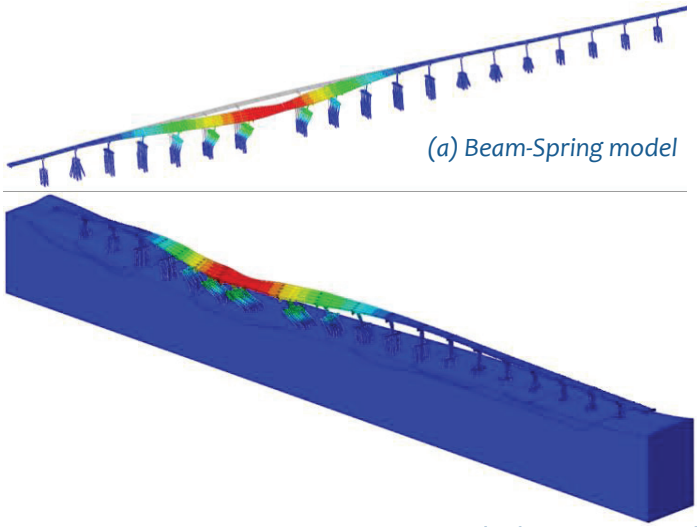

(a) Beam-Spring model

Figure 17: Transverse mode shapes computed

The primary parameters that were manipulated in the both models to match the observed responses were the column and pile stiffnesses. The cross-sectional bending stiffness values had to be reduced to approximately 50% of their nominal values until the measured and predicted responses agreed. This type of reduction is not surprising, in hindsight, for reinforced concrete elements (see, for example, ASCE 41-06, 2006), and similar observations were made in forced vibration experiments and model updating studies on buildings (see, for example, Yu et al., 2009). Another important factor was the use of an accurate value for the mass of the pile-caps.

Figures 18 and 19 display the recorded deck displacements, and nonlinear time-history results at Pier 8 in the longitudinal (Channels 11) and trans-verse (Channels 10) directions. The agreement between the recorded and computed motions is very good.

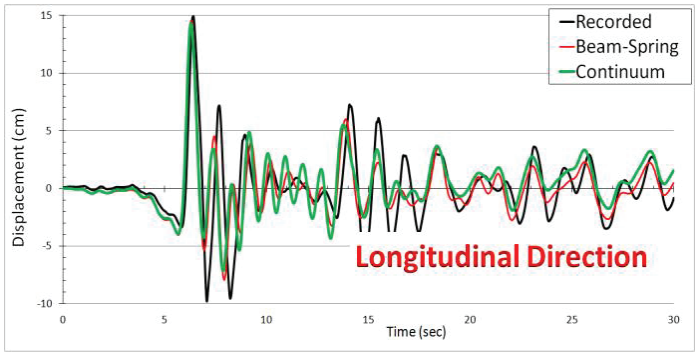

Figure 18: Comparison of beam-springs and continuum models with measured longitudinal bridge responses (CH 11) at Pier 8

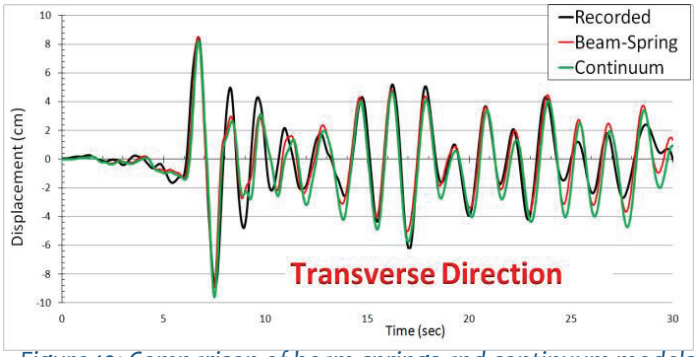

Figure 19: Comparison of beam-springs and continuum models with measured transverse bridge responses (CH 10) at Pier 8

For both models, the calibration of the pile and column stiffnesses (using reduced/cracked values), and an accurate representation of the mass of the pile-caps were essential to capturing the observed response. For the sake of brevity, details of the calibration (finite element model updating) procedure were omitted, and results for only a few recorded channels are presented in this study.

8 CONCLUSIONS

This paper presented two detailed models, the so called the "beam-spring" model and "coupled-continuum" model of the bridge. Both models were calibrated using mode shapes, fundamental periods and the recorded bridge response during the 2010 Ferndale earthquake. Within the framework of the beam-spring model the bridge super-structure, the columns and the foundation elements are modeled as a frame element with idealized cracked moment of inertia, effective mass and stiffness. Macroelements (nonlinear springs, gap elements, etc.) were used to represent the response of the abutment backfill and the soil surrounding the piles. The continuum FE model had a more refined accurate representation of the bridge structure and the supporting pile foundation and inelastic soil medium. The analysis results of both models show good agreement with recorded data. However, the continuum model opens up other modeling opportunities such as realistic simulations of earthquake-induced damage to the pile foundations due to lateral spreading of liquefiable soils. Moreover, as a result of modeling a fully integrated soil and superstructure together, the realistic induced damage on superstructure including cracking, failure of joints, and failure of reinforcement due to seismic loads can be efficiently simulated.

9 REFERENCES

ASCE 41-06—American Society of Civil Engineers (2006). Seismic Rehabilitation of Existing Buildings, Standards ASCE/SEI 41-06, ASCE, Washington, D.C., 2000.

API—American Petroleum Institute (1993), Recommended Practice and Planning, Designing, and Constructing Fixed Offshore Platforms – Working Stress De-sign (RP 2A-WSD), Washington, D.C.

Boulanger RW, Curras CJ, Kutter, BL, Wilson DW, Abghari A (1999). "Seismic soil–pile–structure interaction experiments and analyses." J. Geotech. Geoen-viron. Eng., 125(9), 750–759.

Caltrans (1968), As-Built Drawings, Samoa Channel Bridge Structures. California Dept. of Transportation, Sacramento, CA

Caltrans (2002), As-Built Drawings, Seismic Retrofit of the

Samoa Channel Bridge. California Dept. of Transportation, Sacramento, CA.

Caltrans (2010). Seismic Design Criteria, Version1.6. Ca-lif. Dept. of Transportation, Sacramento, CA.

CSMIP (2012). California Strong Motion Instrumentation Program, http://www.conservation.ca.gov/cgs/smip.

ENSOFT Inc. (2013). ENSOFT DynaPile (v2.0), A Pro-gram for the Analysis of Pile Foundations Under Dy-namic Loading http://www.ensoftinc.com

Hipley P. and Huang M, (1997). "Caltrans/CSMIP bridge strong motion instrumentation," Second National Seismic Conference on Bridge and Highways, Sacra-mento, California.

Matlock, H. (1970), "Correlation for Design of Laterally Loaded Piles in Soft Clay," 2nd Annual Offshore Technology Conference, Paper No. 1204.

Safak, E. (2006). "Time-domain representation of frequency-dependent foundation impedance functions," Soil Dynamics & Earthquake Engineering, 26(1): 65-70.

Shamsabadi, A., Khalili-Tehrani, P., Stewart, J.P. and Taciroglu, E. (2010). "Validated Simulation Models for Lateral Response of Bridge Abutments with Typical Backfills," J. Bridge Eng., ASCE, 15(3), 302-311.

Taciroglu E, Rha CS, Wallace JW (2006). "A robust macroelement model for soil-pile interaction under cyclic loads." Journal of Geotechnical & Geoenv. Engineering, ASCE, 132(10), 1304-1314.

TNO DIANA (2013) DIANA (Release 9.5) [Computer program]. Delft, The Netherlands. http://tnodiana.com

Yu E., Wallace J.W. and Taciroglu E. (2007). "Parameter identification of framed structures using an improved finite element model updating method, Part II: Application to experimental data," Earthquake Engineering & Structural Dynamics, 36, 641-660.

Our Online Library

If you have found the articles included within this issue of DIANA ELEMENTS interesting and useful, you will be interest to know that these and a number of other papers related to DIANA Finite Element Analysis are available via our website. Every year both members of our team and clients write a number of articles about Finite Element Analysis, their research and projects involving DIANA. Continuing with our theme of working, listening and helping DIANA users, and also potential users, we have a facility on our website whereby you can see a short abstract of these papers and request a copy if they are available.

You can find this option under "Services" > "Useful Resources" on our website, or use the following link: http://tnodiana.com/Library. In return we ask only one thing - that you register on our website beforehand and provide some brief information about yourself. If you are already registered then you just simply need to log in. To register or login click on the MY ACCOUNT link at the top right of our website and follow the simple instructions to either login or "Create new account".

You will then have access to the current selection of articles, keep an eye on the site for new articles that will be added over the next few months - all courtesy of TNO DIANA BV.

Bright Sparks...

"... every year TNO DIANA welcomes a number of students temporarily into the team. It always proves to be a learning experience for both the students and us!"

Our interns are normally MsC or PhD Students looking for some experience to help write their thesis. In some cases they are post graduate research assistants looking to gain a little more experience in the finite element analysis of stuctures and the theory behind it.

When they leave us they are often heading out in the world - we would like to say Thank You, Congratulations and Good Luck to the the Class of 2014:

- Fernando Sirumbal: MSc student studying numerical modelling of reservoir-dam interaction seismic response using Hybrid Frequency-Time Domain (HFTD) method. During his internship he worked closely with the advanced software development engineers at TNO DIANA.

  After the completion of his internship Fernado worked as a Structural Engineer at Pöyry whilst carrying out research at Universidad Nacional de Ingenieria in his home country of Peru. Fernando is now studying for a PhD at Imperial College London.

- Joost van Ballegooie: MSc student studying Civil Engineering. Whilst at TDBV Joost worked on a comparison between stiffness adaptation and sequential linear performance. Both procedures were studied, described and evaluated with benchmark tests.

  Joost is now working at Royal Haskoning DHV.

- Djamal Labib: MSc student studying the nonlinear dynamic behaviour of a scaled 3-storey RC structure, on a shaking table, for the international benchmark SMART2013 in Paris. Together with TNO DIANA staff, Djamal travelled to Paris to present the results in November.

  Djamal is now following further courses at the Technical University of Delft.

- Alex Sangers: MSc student in Applied Mathematics, Numerical Analysis. Alex worked on efficiency optimisation of the DIANA Interative linear equation solver, in particular models with large variations in the stiffness of elements and model interface elements.

  Alex is currently working as a Junior Scientist at the Dutch research insititute TNO in the department of Performance of Network and Systems.

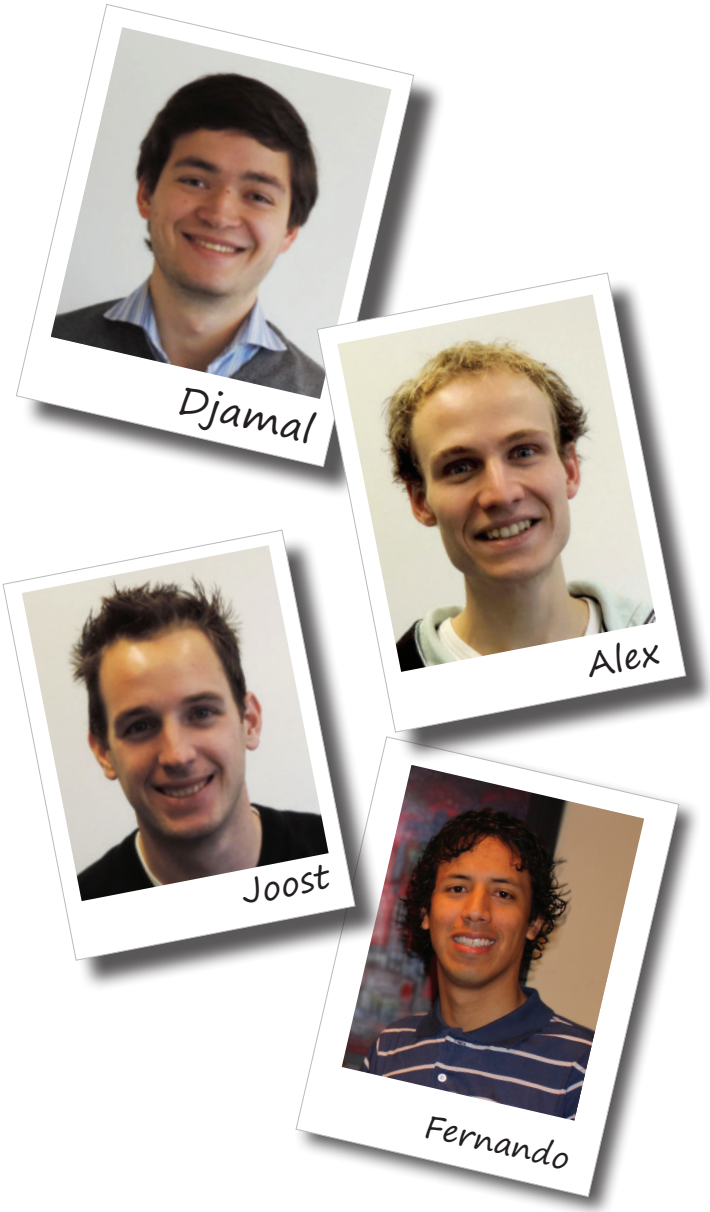

Training & Webinars for Everyone

At TNO DIANA BV we like to pride ourselves on being able to reach out to all of our users and followers world-wide.

With this in mind, throughout 2014, we have run a number of courses in-house here at Delft for both clients and members of the public, as well as visiting clients and providing training on location around the world.

For those with restricted budgets and/or limited time - we have also provided regular webinars on key topics which are free of charge and open to everyone.

2014

In 2014 we were delighted to be able to introduce several guest lecturers who were able to explain how DIANA is being used across both commercial and research projects in many engineering disciplines.

In 2014 topics included:

- Design checks and prediction of cracks using new applications in DIANA
- Technical notes on the simulation of tunnel linings, hosted by Dr Mehdi Bakhshi, Senior Tunnel Designer at AECOM New York
- Dynamic analysis of structures with DIANA
- Seismic analysis of dams using the HFTD method, hosted by Fernando Sirumbal at the end of his Internship at TNO DIANA BV
- Analysis of pre-stressed reinforced concrete bridges
- Simulation aided damage assessment in concrete structures, hosted by Dr Kamyab Zandi of the Swedish Cement and Concrete Research Insititute, part of Chalmers University

In addition, our CEO, Dr Gerd-Jan Schreppers has hosted two sessions detailing the new functionality in DIANA 9.5 and 9.6. And our regular "Introduction to DIANA" webinar has been run throughout the year in a number of languages.

2015

In 2015 we will continue with a range of exciting topics and presenters.

TNO DIANA BV Dedicated technical courses in 2015:

- Nonlinear behaviour of reinforced concrete structures
- Finite Element Analysis for geotechnical applications
- Analysis of various dam structures with DIANA
- Finite Element Analysis for oil and gas applications

We will also organize a series of short and technical workshops on:

- Dynamic analysis of structures
- Python scripting for DIANA applications
- DIANA applications for masonry structures
- DIANA solution for fiber reinforced concrete structures

And as usual you can follow our free technical webinars based on various topics such as:

- Introduction to DIANA for new users
- Simulation of fully coupled soil-structure-interaction analysis
- An overview of the analysis of large dams
- Analysis and assessment of bridge structures
- Piled raft foundation solutions
- Failure mechanisms of concrete structures
- Simulation and assessment of masonry and historical structures
- DIANA solutions for the dynamic analysis of super-structures
- TBM tunneling and technical recommendations
- And many more…

Signup is simple and you can join via your PC, laptop, tablet or even smart phone (assuming you have an internet connection!).

To ensure that you hear about upcoming events, sign up for our monthly **newsletter**, or simply keep an eye on our website.

We look forward to you joining us in 2015.